

# Corneal immune cells as a biomarker of inflammation in multiple sclerosis: a longitudinal study

Ioannis N. Petropoulos, Karen John, Fatima Al-Shibani, Georgios Ponirakis, Adnan Khan, Hoda Gad, Ziyad R. Mahfoud, Heba Altarawneh, Muhammad Hassan Rehman, Dhabia Al-Merekhi, Pooja George, Faiza Ibrahim, Reny Francis, Beatriz Canibano, Dirk Deleu, Ahmed El-Sotouhy, Surjith Vattoth, Mark Stettner<sup>ID</sup>, Ahmed Own, Ashfaq Shuaib, Naveed Akhtar, Saadat Kamran<sup>ID</sup> and Rayaz A. Malik<sup>ID</sup>

## Abstract

**Background:** Corneal immune cells (ICs) are antigen-presenting cells that are known to increase ocular and systemic inflammatory conditions.

**Objective:** We aimed to assess longitudinal changes in corneal IC in patients with multiple sclerosis (MS) and relation to disability and ongoing treatment.

**Design:** Prospective observational study conducted between September 2016 and February 2020.

**Methods:** Patients with relapsing-remitting MS (RRMS) ( $n=45$ ) or secondary progressive MS (SPMS) ( $n=15$ ) underwent corneal confocal microscopy (CCM) at baseline and 2-year follow-up for estimation of corneal IC density [dendritic cells with (DCF) (cells/mm<sup>2</sup>) or without nerve fiber contact (DCP); and non-dendritic cells with (NCF) or without nerve fiber contact (NCP)]. Optical coherence tomography, neuroimaging, and disability assessments were additionally performed. Healthy controls ( $n=20$ ) were assessed at baseline.

**Results:** In both RRMS and SPMS compared to controls, DCP ( $p < 0.001$  and  $p < 0.001$ , respectively) and DCF ( $p < 0.001$  and  $p = 0.005$ ) were higher and NCF ( $p = 0.007$  and  $p = 0.02$ ) was lower at baseline. DCP showed excellent performance in identifying patients with MS (sensitivity/specificity = 0.88/0.90) followed by DCF (0.80/0.75) and NCF (0.80/0.85). At follow-up compared to baseline, DCP ( $p = 0.01$ ) was significantly reduced, and NCP ( $p = 0.004$ ) and NCF ( $p = 0.04$ ) were increased. Subgroup analysis showed that baseline NCP and NCF were significantly higher ( $p = 0.04$ – $0.05$ ) in patients who switched disease-modifying treatment, and baseline NCP ( $p = 0.05$ ) was higher in patients on interferon.

**Conclusion:** Baseline and change in corneal IC were related to axonal degeneration and treatment status. Evaluation of corneal IC using CCM may allow an assessment of ongoing inflammation, disease progression, and the effect of treatment in MS.

**Keywords:** biomarker, corneal confocal microscopy, inflammation, multiple sclerosis, neurodegeneration

Received: 5 June 2023; revised manuscript accepted: 12 September 2023.

## Introduction

Multiple sclerosis (MS) is a chronic inflammatory, central demyelinating disorder, and axonal

loss is a key determinant of disease progression. Neuroinflammation is present in all stages of the disease, due to activation of the innate and

*Ther Adv Neurol Disord*

2023, Vol. 16: 1–16

DOI: 10.1177/  
17562864231204974

© The Author(s), 2023.  
Article reuse guidelines:  
sagepub.com/journals-  
permissions

Correspondence to:  
**Rayaz A. Malik**  
Weill Cornell Medicine-  
Qatar of Cornell University,  
Research Division, Qatar  
Foundation, Education  
City, Al-Luqta street, Doha  
24144, Qatar  
ram2045@qatar-med.  
cornell.edu

**Ioannis N. Petropoulos**  
**Karen John**  
**Fatima Al-Shibani**  
**Georgios Ponirakis**  
**Adnan Khan**  
**Hoda Gad**  
**Heba Altarawneh**  
**Muhammad Hassan**  
**Rehman**  
**Dhabia Al-Merekhi**  
Division of Research, Weill  
Cornell Medicine, Doha,  
Qatar

**Ziyad R. Mahfoud**  
Division of Medical  
Education, Weill Cornell  
Medicine, Doha, Qatar  
Division of Epidemiology,  
Department of Population  
Health Sciences, Weill  
Cornell Medicine, New  
York, NY, USA

**Pooja George**  
**Faiza Ibrahim**  
**Reny Francis**  
**Beatriz Canibano**  
**Dirk Deleu**  
**Ahmed El-Sotouhy**  
**Ahmed Own**  
**Naveed Akhtar**  
**Saadat Kamran**  
Neuroscience Institute,  
Hamad Medical  
Corporation, Doha, Qatar

**Surjith Vattoth**  
Neuroscience Institute,  
Hamad Medical  
Corporation, Doha, Qatar  
Department of Radiology,  
University of Arkansas for  
Medical Sciences, Little  
Rock, AR, USA

**Mark Stettner**  
Department of  
Neurology and Center  
for Translational Neuro-  
and Behavioral Sciences  
(C-TNBS), University  
Hospital Essen, Essen,  
Germany



**Ashfaq Shuaib**

Neuroscience Institute,  
Hamad Medical  
Corporation, Doha, Qatar

Department of Medicine,  
University of Alberta,  
Edmonton, Qatar

\*Joint last authors

adaptive immune systems.<sup>1</sup> Neuropathological hallmarks of inflammation include multifocal white matter demyelinating lesions,<sup>2</sup> impaired blood–brain barrier function,<sup>3</sup> leptomeningeal inflammation,<sup>4</sup> and lymphocyte infiltration in the brain parenchyma.<sup>5</sup> Newer methods such as quantitative gadolinium magnetic resonance imaging (MRI) scanning,<sup>6</sup> T2 Fluid-Attenuated Inversion Recovery (FLAIR) MRI,<sup>7</sup> susceptibility imaging,<sup>8</sup> positron emission tomography,<sup>9</sup> and magnetic resonance spectroscopy<sup>10</sup> can assess inflammation. Although T2-FLAIR MRI with gadolinium enhancement can be used to quantify inflammatory activity in addition to white matter lesion counts, the use of contrast should be justified.<sup>11</sup> Positron emission tomography studies are useful to assess chronic microglial activation but have low specificity due to poor spatial resolution and lack of microglia-specific radioligands.<sup>12</sup> Magnetic resonance spectroscopy of brain myoinositol may act as a biomarker of astrogliosis, but its specificity is questionable as it is also expressed in cells other than astrocytes.<sup>13</sup>

Surrogate endpoints of neurodegeneration have attracted considerable interest to monitor and predict MS progression. Optical coherence tomography (OCT) has shown retinal nerve fiber layer (RNFL) thinning in MS, but this may be attenuated during acute optic neuritis (ON).<sup>14</sup> We and others have used corneal confocal microscopy (CCM) to show a corneal axonal loss, independent of ON and related it to the severity of MS.<sup>15–21</sup> Corneal plasmacytoid dendritic immune cells (ICs) are bone marrow-derived antigen-presenting cells responsible for inducing primary immune responses and establishing immunologic memory *via* antigen capture and T-cell stimulation, respectively.<sup>22</sup> Recent experimental evidence has shown that corneal IC plays an important role in corneal nerve degeneration.<sup>23</sup> Alterations in their density, morphology, and distribution have been demonstrated in Sjogren's syndrome,<sup>24</sup> rheumatoid arthritis,<sup>25</sup> systemic lupus erythematosus,<sup>26</sup> and chronic inflammatory demyelinating polyradiculoneuropathy.<sup>27</sup> In MS, Bitirgen *et al.* first showed increased dendritic cell density in patients with relapsing-remitting MS (RRMS),<sup>15</sup> with a significant increase in patients with worsening disability at follow-up.<sup>16,28</sup> Khan *et al.*<sup>29</sup> demonstrated increased corneal IC density in patients with RRMS, to a lesser extent in secondary progressive MS (SPMS) and clinically isolated syndrome, and showed an association with cognitive function and

neurological disability. In the present study, we have prospectively assessed alterations in corneal IC density in relation to corneal and retinal axonal morphology, disease-modifying treatment, MRI abnormality, and neurological disability.

## Methods

### *Study participants and setting*

This is a prospective, observational study conducted in Doha, Qatar (September 2016–2020). Patients with RRMS ( $n=45$ ) and SPMS ( $n=15$ ) underwent assessment of neurological disability, cranial MRI, and CCM at baseline and follow-up. Age-matched, healthy controls ( $n=20$ ) were assessed at baseline (Figure 1). Reporting of results in this study followed the STROBE guidelines. Inclusion criteria were MS diagnosis<sup>30</sup> and age 18–75 years. Exclusion criteria were the presence of ophthalmic disease, active ON (<6 months from diagnosis of ON episode), and history of ophthalmic surgery. Patients with comorbidities associated with peripheral neuropathy were also excluded.

### *Clinical assessments*

The expanded disability status scale (EDSS) was used to rate neurological impairment. The MS severity score (MSSS) was calculated from EDSS and MS duration.<sup>31</sup> The number of relapses and annualized relapse rate (ARR) were used as indications of disease activity over time. For the 25-foot walking test (25 FWT), the time was calculated from the starting point until the 25-foot mark. All clinical assessments preceded CCM except for cranial MRI scans, which were performed  $\pm 1$  month from ophthalmic assessments based on availability. Clinical information was obtained from the participant's electronic medical records.

### *Corneal confocal microscopy*

CCM scans (Heidelberg Retinal Tomograph III Rostock Cornea Module, Heidelberg Engineering GmbH, Heidelberg, Germany) were performed as per the established methodology.<sup>32</sup> Based on location (apical cornea) and clarity (i.e. visibility of subbasal nerves without pressure lines), eight non-overlapping images/participants were analyzed by the same examiner with CCMetrics/ACCMetrics.<sup>27,32</sup> The corneal nerve parameters measured were corneal nerve fiber density (CNFD) (fibers/mm<sup>2</sup>), corneal nerve branch density

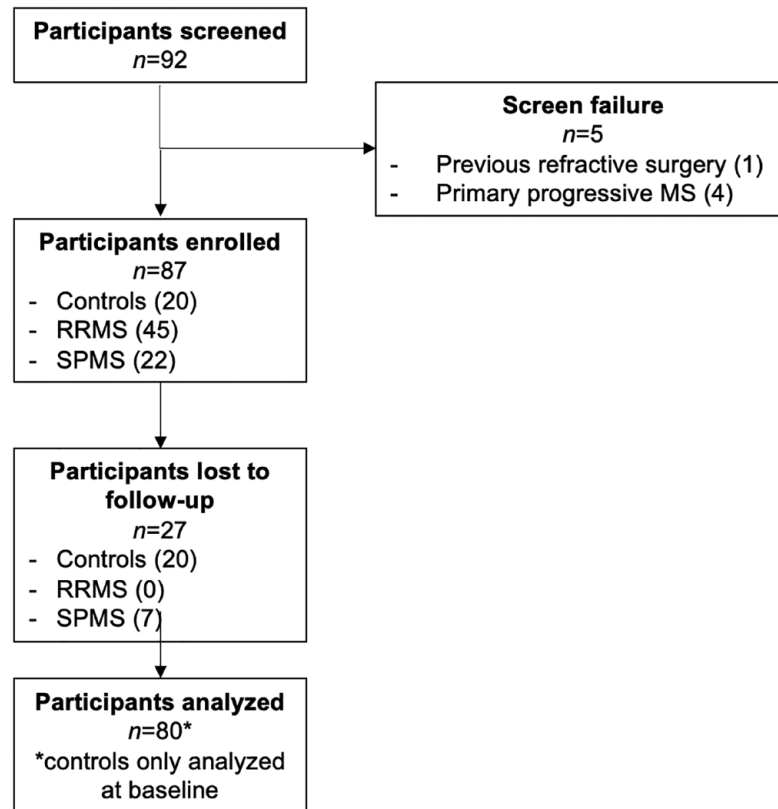


**Figure 1.** Flow diagram of individuals at each stage of the study.

(CNBD) (branches/mm<sup>2</sup>), corneal nerve fiber length (CNFL) (mm/mm<sup>2</sup>), and corneal nerve fractal dimension analysis (CNFrD). Corneal ICs were assessed on the same images.<sup>27,33</sup> Cells were classified into dendritic cells (DC) and non-dendritic cells based on morphology, and the corneal IC parameters measured were dendritic cells with fiber contact (DCF) (cells/mm<sup>2</sup>), without fiber contact (DCP) (cells/mm<sup>2</sup>), and non-dendritic cells with fiber contact (NCF) (cells/mm<sup>2</sup>), and without fiber contact (NCP) (cells/mm<sup>2</sup>) (Figure 2). The CCM parameters are presented as an average of analyzed images per participant. All CCM examiners were masked to the subtype of MS, clinical, and MRI examination results. Intra-rater reliability of corneal IC quantification was assessed by re-analyzing images of  $n=16$  (20%) patients (four healthy controls; nine patients with RRMS; and three patients with SPMS).

#### *Optical coherence tomography*

Peripapillary RNFL thickness measurements were performed with a spectral-domain OCT

(Spectralis OCT, Heidelberg Engineering GmbH, Heidelberg, Germany) under the same lighting conditions without pupil dilation. RNFL measurements were performed using circular scans with the eye tracker activated to minimize motion artifacts. All RNFL scans in this study were performed in high-speed mode, and a signal strength of  $\geq 20/30$  was set as the minimum acceptable quality. Follow-up RNFL scans were performed using the 'progression' function. The built-in segmentation function was used to calculate peripapillary RNFL thickness.

#### *Statistical analysis*

IBM SPSS Statistics for Mac, version 26 (IBM Corp., Armonk, NY, USA) and Prism 9 for Mac, Version 9.4.1 (GraphPad Software, San Diego, CA, USA) were used for the statistical analysis and graphic illustrations in this study. This study was originally powered to detect differences in corneal nerve morphology in patients with MS compared to controls.<sup>28</sup> Post hoc power calculation using univariate analysis of variance with

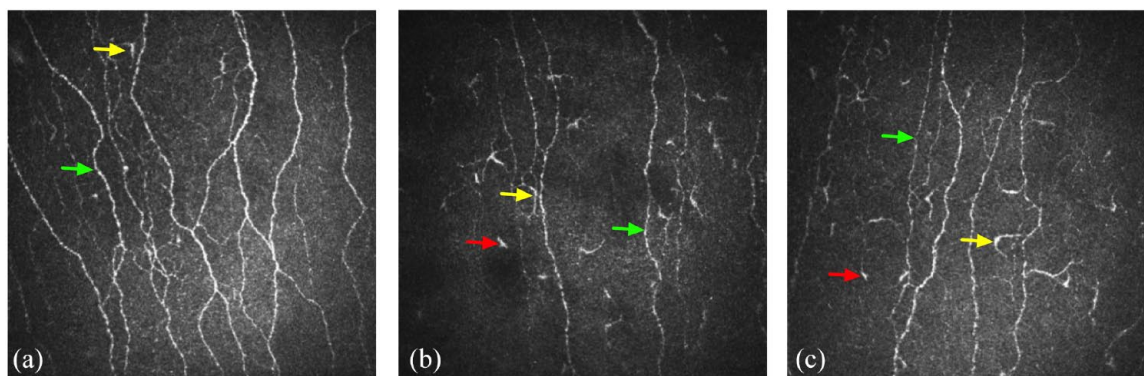


**Figure 2.** CCM images of the subbasal nerve plexus from a healthy control (a), a patient with RRMS at baseline (b), and the same patient with RRMS at follow-up (c). Yellow arrows denote dendritic cells with/without contact with the nerve fibers and red arrows denote non-dendritic cells with/without contact with the nerve fibers. Green arrows denote corneal axons. CCM, corneal confocal microscopy; RRMS, relapsing-remitting multiple sclerosis.

baseline DCP as the dependent variable and patient status as the fixed factor showed that a sample of  $n=80$  participants (effect size = 0.17,  $p < 0.001$ ) provides 97.8% power with  $\alpha=0.05$ . Continuous data were tested for normality using a Shapiro–Wilk test ( $p > 0.05$ ) and relevant histograms (Q–Q plots). Baseline and follow-up CNFD, CNBD, CNFL, and RNFL followed a normal distribution, while baseline and follow-up EDSS, MSSS, ARR, number of relapses, 25 FWT, DCP, DCF, NCF, and NCP did not follow a normal distribution. An unpaired  $t$ -test or nonparametric Mann–Whitney  $U$  test was used for comparisons between the MS group and healthy controls; a paired  $t$ -test was used for comparisons between MS patients at baseline and follow-up. One-way ANOVA (post hoc Bonferroni) or nonparametric Kruskal–Wallis (Dunn’s test for multiple comparisons correction) was used for comparisons between controls and MS subtypes. Receiver operating characteristic (ROC) curve analysis was performed to assess the diagnostic performance of corneal IC measurements. Cutoff points that balanced sensitivity and specificity were selected based on Youden’s index. Spearman’s correlation analysis was performed to assess the relationship between corneal IC measurements, and demographic, clinical, corneal, retinal nerve measurements, and time. The intra-class correlation coefficient [95% confidence interval (CI),  $p$  Value] was used to assess the intra-rater reliability of corneal IC analysis. Typically, ICC values  $\geq 0.8$  are considered very

good and  $\geq 0.9$  indicate excellent reliability. Continuous parametric data are expressed as (mean difference, 95% CI of differences,  $p$  Value) and nonparametric data as (median difference, 95% CI of differences,  $p$  Value). The reported  $p$  values are two-sided and a  $p \leq 0.05$  was considered significant.

#### Data availability

All anonymized, individual-level data used in this manuscript are available to qualified researchers by direct request to the corresponding author. All interested applicants will be asked to sign a data transfer agreement according to institutional regulations prior to receiving any data.

## Results

### Baseline demographic and clinical results

There was no significant difference in age [controls *versus* RRMS ( $-2.5, -4.0-3.0, p=1.0$ ); controls *versus* SPMS ( $-5.5, -2.0-10.0, p=0.59$ ); RRMS *versus* SPMS ( $-3.0, -2.0-9.0, p=0.53$ )] or sex between controls and patients with MS. Patients with SPMS, compared to RRMS, had a significantly longer time since diagnosis of MS ( $-4.0, -6.0$  to  $-1.0, p=0.005$ ); more relapses ( $-3.0, -1.0$  to  $-3.0, p < 0.001$ ), greater ARR ( $-1.52, -2.06$  to  $-0.62, p < 0.001$ ), EDSS ( $-4.0, -5.0$  to  $-2.0, p < 0.001$ ), and MSSS ( $-4.27, -5.55$  to  $-2.56, p < 0.001$ ) (Table 1).

**Table 1.** Baseline demographic, clinical, and ophthalmic characteristics.

Parameters	Controls	RRMS	SPMS	<i>p</i> Value
<i>n</i> (%)	20	45 (75)	15 (25)	–
Age (years)	33.50 ± 2.10	36.0 ± 1.29	39.0 ± 2.31	0.35
Sex, <i>n</i> (% women)	14 (70)	30 (66)	10 (66)	>0.99
Time since diagnosis (years)	–	6.0 ± 0.50	10.0 ± 0.98	0.005
ON history, <i>n</i> (%)	0 (0)	22 (49)	8 (53)	–
Number of relapses	–	1.0 ± 0.18	4.0 ± 0.48	<0.001
ARR	–	0.51 ± 0.12	2.03 ± 0.44	<0.001
EDSS	–	0 ± 0.12	4.0 ± 0.66	<0.001
MSSS	–	0.67 ± 0.20	4.94 ± 0.84	<0.001
25 FWT (s)	3.80 ± 0.19	6.0 ± 0.49 <sup>a</sup>	8.59 ± 2.43 <sup>a</sup>	<0.001
DMT use, <i>n</i> (%)	–	35 (78)	15 (100)	–
Beta interferon, <i>n</i> (%)	–	15 (33)	2 (13)	–
Fingolimod, <i>n</i> (%)	–	5 (11)	6 (40)	–
Dimethyl fumarate, <i>n</i> (%)	–	8 (18)	6 (40)	–
Other <sup>‡</sup> , <i>n</i> (%)	–	7 (16)	1 (7)	–
CNFD (fibers/mm <sup>2</sup> )	35.73 ± 1.37	32.37 ± 1.12	29.47 ± 1.93 <sup>a</sup>	0.04
CNBD (branches/mm <sup>2</sup> )	102.67 ± 7.09	129.96 ± 7.47	120.03 ± 14.79	0.11
CNFL (mm/mm <sup>2</sup> )	24.39 ± 0.92	22.85 ± 0.78	21.13 ± 1.49	0.17
CNFrD	1.51 ± 0.005	1.47 ± 0.004 <sup>a</sup>	1.46 ± 0.01 <sup>a</sup>	<0.001
RNFL (μm)	97.50 ± 2.72	89.07 ± 1.77	76.01 ± 3.98 <sup>a,b</sup>	<0.001
DCP (cells/mm <sup>2</sup> )	1.04 ± 0.28	26.04 ± 7.72 <sup>a</sup>	33.33 ± 9.68 <sup>a</sup>	<0.001
DCF (cells/mm <sup>2</sup> )	3.39 ± 0.54	10.94 ± 1.59 <sup>a</sup>	11.72 ± 2.85 <sup>a</sup>	<0.001
NCP (cells/mm <sup>2</sup> )	3.0 ± 1.75	7.14 ± 1.62	12.50 ± 2.95 <sup>a</sup>	0.04
NCF (cells/mm <sup>2</sup> )	9.77 ± 2.49	1.04 ± 1.63 <sup>a</sup>	1.56 ± 1.27 <sup>a</sup>	<0.001

Data are expressed as mean or median ± standard error of mean depending on their distribution (parametric or nonparametric) or as *n* (%) where applicable. For multiple comparisons, The *p* value corresponds to the overall *p* Value of the test (one-way ANOVA Fisher's; or Kruskal-Wallis). CNFD: significantly different in SPMS *versus* controls (*p* < 0.001). CNFrD: significantly different in RRMS *versus* controls (*p* < 0.001); and in SPMS *versus* controls (*p* < 0.001). RNFL: significantly different in RRMS *versus* controls (*p* = 0.051); in SPMS *versus* controls (*p* < 0.001) and in SPMS *versus* RRMS (*p* = 0.003). DCP: significantly different in RRMS *versus* controls (*p* < 0.001); and in SPMS *versus* controls (*p* = 0.02). DCF: significantly different in RRMS *versus* controls (*p* < 0.001); and in SPMS *versus* controls (*p* = 0.005). NCF: significantly different in RRMS *versus* controls (*p* = 0.007); and in SPMS *versus* controls (*p* = 0.02).

<sup>a</sup>Significantly different from controls.

<sup>b</sup>Significantly different from RRMS.

Other medications: <sup>‡</sup>Teriflunomide (*n* = 6), natalizumab (*n* = 1), alemtuzumab (*n* = 1).

ARR, annualized relapse rate; CNBD, corneal nerve branch density; CNFD, corneal nerve fiber density; CNFL, corneal nerve fiber length; CNFrD, corneal nerve fractal dimension analysis; DCF, dendritic cells with fiber contact; DCP, dendritic cells without fiber contact; DMT, disease-modifying therapy; EDSS, expanded disability status scale; FWT, foot walking test; MS, multiple sclerosis; MSSS, multiple sclerosis severity score; NCF, non-dendritic cells with fiber contact; NCP, non-dendritic cells without fiber contact; ON, optic neuritis; RNFL, retinal nerve fiber layer; RRMS, relapsing-remitting multiple sclerosis; SPMS, secondary progressive multiple sclerosis; s, seconds.

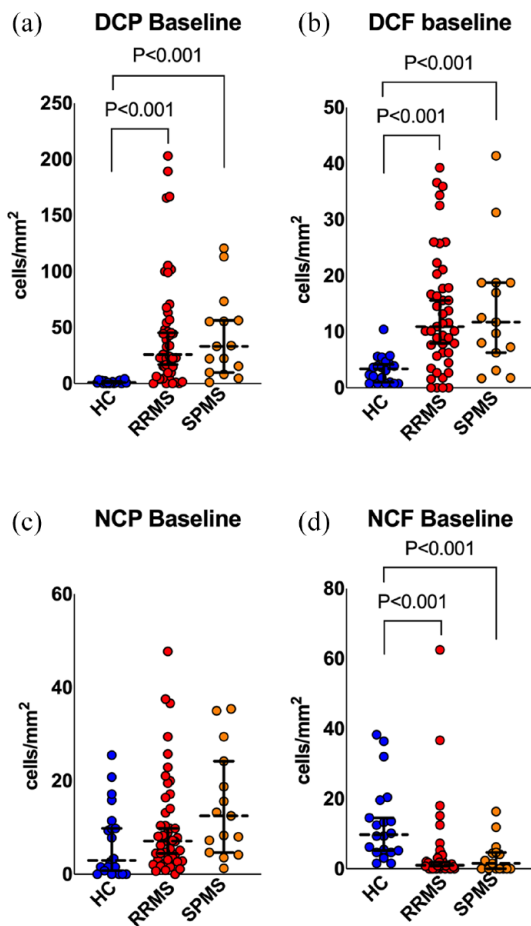


**Figure 3.** Scatter plots of baseline corneal immune cell density. Graphs represent the median and 95% confidence interval (dashed and continuous black lines, respectively) overlaid with the full data range for DCP (a), DCF (b), NCP (c), and NCF (d). Data circles represent controls (blue), patients with RRMS (red), and SPMS (yellow).

DCF, dendritic cells with fiber contact; DCP, dendritic cells without fiber contact; NCF, non-dendritic cells with fiber contact; NCP, non-dendritic cells without fiber contact; RRMS, relapsing-remitting multiple sclerosis; SPMS, secondary progressive multiple sclerosis.

#### Baseline corneal ICs

**Healthy controls versus RRMS.** DCP (25.0, 15.62–44.35,  $p < 0.001$ ) and DCF (7.56, 4.90–12.50,  $p < 0.001$ ) were higher and NCF (–8.73, –11.72 to –4.17,  $p < 0.001$ ) was lower in patients with RRMS compared to healthy controls at baseline (Table 1 and Figure 3).

**Healthy controls versus SPMS.** DCP (32.29, 14.58–54.43,  $p < 0.001$ ), DCF (8.34, 3.91–14.62,  $p < 0.001$ ), and NCP (9.51, 1.23–13.28,  $p = 0.02$ )

were higher and NCF (–8.21, –13.28 to –3.12,  $p < 0.001$ ) was lower in patients with SPMS compared to healthy controls at baseline (Table 1 and Figure 3).

**RRMS versus SPMS.** There was no significant difference in corneal IC parameters between RRMS and SPMS subgroups at baseline (Table 1 and Figure 3).

**ROC curve analysis.** DCP showed excellent performance to identify patients with MS [area under the curve (AUC)=0.92, 95% CI=0.85–0.98,  $p < 0.001$ , sensitivity/specificity=0.88/0.95, likelihood ratio=17.67 using DCP > 3.78 cells/mm<sup>2</sup> as cutoff point] followed by DCF (0.83, 0.75–0.92,  $p < 0.001$ , 0.80/0.75, 3.20, DCF > 4.32 cells/mm<sup>2</sup>); NCF (0.86, 0.78–0.94,  $p < 0.001$ , 0.80/0.85, 5.33, NCF < 4.58 cells/mm<sup>2</sup>); and NCP (0.66, 0.51–0.81,  $p = 0.03$ , 0.78/0.55, 1.74, NCP > 3.48 cells/mm<sup>2</sup>) (Figure 4).

#### Follow-up demographic and clinical results

The average follow-up time was 18.26 ± 4.27 months. In patients with RRMS at follow-up, there was a significant increase in the number of relapses (0.2, 0.06–0.34,  $p = 0.008$ ) and ARR (0.04, 0.04–0.23,  $p = 0.008$ ) and a significant decrease in MSSS (–0.07, –0.18 to –0.03,  $p < 0.001$ ) and the 25 FWT (–1.50, –2.70 to –0.08,  $p = 0.02$ ). In patients with SPMS at follow-up, there was a significant increase in the number of relapses (0.4, 0.12–0.68,  $p = 0.03$ ) and ARR (0.12, 0.07–0.44,  $p = 0.03$ ) (Table 2).

#### Follow-up corneal immune cells

**Multiple sclerosis.** In patients with MS, there was a significant reduction in DCP (–9.81, –29.22 to –4.74,  $p = 0.01$ ) and a significant increase in NCP (4.18, 3.46–22.1,  $p = 0.004$ ) and NCF (0.96, –0.82–5.31,  $p = 0.04$ ) at follow-up compared to baseline (Table 2 and Figure 5). There was no significant correlation between follow-up time and the difference between baseline and follow-up DCP ( $r = -0.07$ , –0.32 and 0.20,  $p = 0.62$ ), DCF ( $r = -0.03$ , –0.29–0.24,  $p = 0.83$ ), NCP ( $r = 0.01$ , –0.25–0.27,  $p = 0.92$ ), and NCF ( $r = -0.1$ , –0.35–0.17,  $p = 0.46$ ).

**Relapsing-remitting multiple sclerosis.** In patients with RRMS, there was a significant reduction in DCP [–9.80, –30.81 to –3.30,

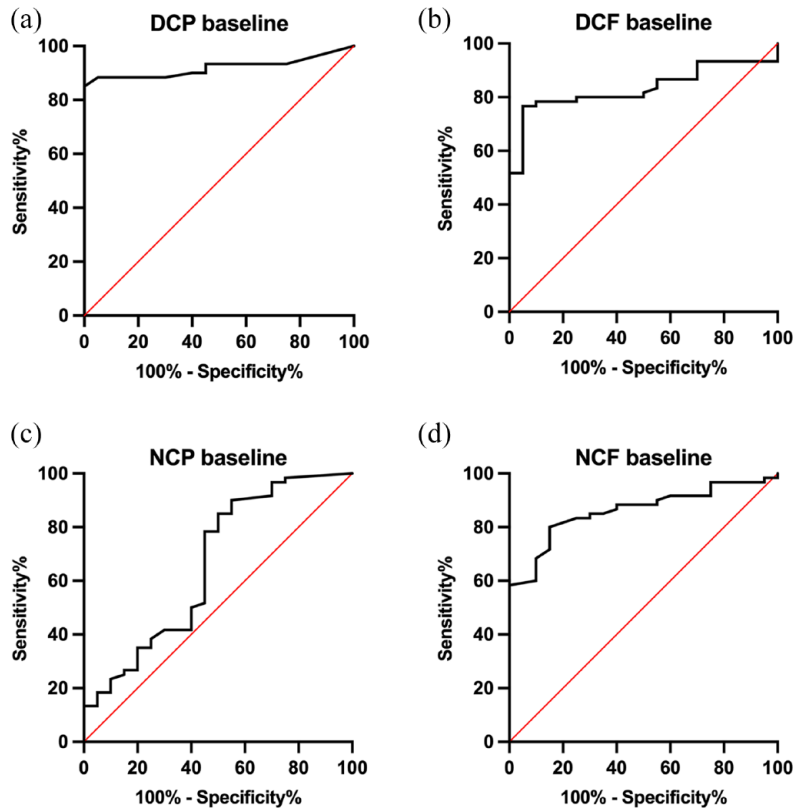


**Figure 4.** Receiver operating characteristics curve analysis of baseline DCP (a), DCF (b), NCP (c), and NCF (d) (all shown as black lines) with reference line (red line) to assess their ability to distinguish between controls and patients with MS.

DCF, dendritic cells with fiber contact; DCP, dendritic cells without fiber contact; NCF, non-dendritic cells with fiber contact; NCP, non-dendritic cells without fiber contact; MS, multiple sclerosis.

$p=0.02$ ] and a significant increase in NCP [1.49, 2.97–25.90,  $p=0.01$ ] at follow-up compared to baseline (Table 2).

*Secondary progressive multiple sclerosis.* In patients with SPMS, there was no significant change in DCP, DCF, NCP, and NCF at follow-up compared to baseline (Table 2).

#### Subgroup analysis

*Corneal ICs in relation to corneal nerve parameters.* Patients with MS were classified according to their baseline status into patients with low corneal axonal density based on a CNFD, CNBD, or CNFL lower than the 25th percentile (CNFD < 27.08 fibers/mm<sup>2</sup>; CNBD < 82.42 branches/mm<sup>2</sup>; or CNFL < 19.32 mm/mm<sup>2</sup>). Patients with low baseline CNFD ( $n=14$ ) compared to all other patients ( $n=46$ ) had significantly higher EDSS (1.50, 0–3.0,  $p=0.02$ ), MSSS

(3.01, 0.20–4.47,  $p=0.02$ ) and DCP at baseline (32.29, 0–76.0,  $p=0.05$ ), and significantly higher EDSS (1.50, 0–2.50,  $p=0.05$ ), ARR (0.91, 0–1.53,  $p=0.05$ ), and DCP (32.59, 3.56–47.16,  $p=0.01$ ) at follow-up [Figure 6(a)–(c)]. Patients with low baseline CNBD ( $n=15$ ) had significantly higher DCP (32.26, 10.16–45.05,  $p<0.001$ ) and DCF (2.22, 0–7.2,  $p=0.05$ ) at follow-up [Figure 6(d)–(f)]. Patients with low baseline CNFL ( $n=15$ ) had significantly higher DCP at follow-up (32.26, 8.04–44.82,  $p=0.002$ ) [Figure 6(g)–(i)].

*Corneal IC in relation to a new clinically documented relapse at follow-up.* Patients with a new relapse ( $n=13$ ) compared to patients without a new relapse ( $n=47$ ) at follow-up had a significantly higher baseline EDSS (0.50, 0–1.50,  $p=0.02$ ), MSSS (1.77, 0.10–2.28,  $p=0.04$ ), and DCP (25.5, 0–48.21,  $p=0.05$ ) and follow-up MSSS (0.46, 0.05–0.71,  $p=0.03$ ), ARR (1.31,

**Table 2.** Baseline and follow-up demographic, clinical, and ophthalmic characteristics.

Parameters	RRMS (n = 45)			SPMS (n = 15)		
	Baseline	Follow-up	p Value	Baseline	Follow-up	p Value
ON history, n (%)	22 (49)	24 (53)	–	8 (53)	8 (53)	–
Relapses, n	1.07 ± 0.18	1.27 ± 0.20	0.008	3.0 ± 0.49	3.40 ± 0.46	0.03
ARR	0.51 ± 0.12	0.55 ± 0.14	0.008	2.03 ± 0.44	2.15 ± 0.43	0.03
EDSS	0.68 ± 0.13	0.48 ± 0.11	0.08	4.0 ± 0.67	5.0 ± 0.69	0.77
MSSS	0.66 ± 0.21	0.33 ± 0.18	<0.001	4.94 ± 0.84	5.40 ± 0.89	0.15
25 FWT (s)	6.0 ± 0.40	4.20 ± 0.39	0.02	8.40 ± 3.14	3.80 ± 6.91	0.38
DMT use, n (%)	35 (78)	38 (84)	–	15 (100)	13 (86)	–
Beta interferon, n (%)	15 (33)	9 (20)	–	2 (13)	0 (0)	–
Fingolimod, n (%)	5 (11)	7 (16)	–	6 (40)	5 (33)	–
Dimethyl Fumarate, n (%)	8 (18)	12 (26)	–	6 (40)	5 (33)	–
Other <sup>a</sup> , n (%)	7 (16)	10 (22)	–	1 (7)	3 (20)	–
CNFD (fibers/mm <sup>2</sup> )	32.37 ± 1.12	29.10 ± 0.98	0.002	29.47 ± 1.93	27.54 ± 2.94	0.37
CNBD (branches/mm <sup>2</sup> )	129.96 ± 7.47	81.53 ± 5.51	<0.001	120.03 ± 14.79	77.23 ± 12.25	0.007
CNFL (mm/mm <sup>2</sup> )	22.85 ± 0.78	20.69 ± 0.70	0.002	21.13 ± 1.49	20.76 ± 1.97	0.81
CNFrD	1.47 ± 0.004	1.47 ± 0.005	0.25	1.46 ± 0.01	1.47 ± 0.01	0.42
RNFL (μm)	88.81 ± 1.79	87.58 ± 1.79	0.003	77.13 ± 4.49	76.46 ± 4.29	0.16
DCP (cells/mm <sup>2</sup> )	26.04 ± 7.72	15.62 ± 6.19	0.02	33.33 ± 9.68	13.28 ± 8.69	0.25
DCF (cells/mm <sup>2</sup> )	10.94 ± 1.59	9.37 ± 1.83	0.22	11.72 ± 2.85	4.86 ± 2.57	0.30
NCP (cells/mm <sup>2</sup> )	7.14 ± 1.62	9.37 ± 6.04	0.01	12.50 ± 2.95	16.96 ± 6.72	0.30
NCF (cells/mm <sup>2</sup> )	1.04 ± 1.63	6.16 ± 1.27	0.06	1.56 ± 1.27	2.34 ± 4.48	0.99

Data are expressed as mean ± standard error of mean or as n (%) where applicable. p Values have been generated with a paired t-test.

<sup>a</sup>Other medications: Teriflunomide (n=9), natalizumab (n=1), alemtuzumab (n=1), ocrelizumab (n=1), and rituximab (n=1).

ARR, annualized relapse rate; CNBD, corneal nerve branch density; CNFD, corneal nerve fiber density; CNFL, corneal nerve fiber length; CNFrD, corneal nerve fractal dimension analysis; DCF, dendritic cells with fiber contact; DCP, dendritic cells without fiber contact; DMT, disease-modifying therapy; EDSS, expanded disability status scale; FWT, foot walking test; MS, multiple sclerosis; MSSS, multiple sclerosis severity score; NCF, non-dendritic cells with fiber contact; NCP, non-dendritic cells without fiber contact; ON, optic neuritis; RNFL, retinal nerve fiber layer; RRMS, relapsing-remitting multiple sclerosis; SPMS, secondary progressive multiple sclerosis; s, seconds.

0.37–2.03,  $p=0.005$ ), and NCP (9.38, 0.89–15.71,  $p=0.03$ ). Furthermore, patients with a new relapse compared to patients without a new relapse had significantly lower baseline CNFD (–4.76, –9.39 to –0.13,  $p=0.04$ ) and CNFL (–3.41, –6.70 to –0.13,  $p=0.04$ ).

Corneal IC in relation to new gadolinium-enhancing lesions at follow-up. Cranial MRI at follow-up showed that eight patients with MS had new gadolinium-enhancing lesions. Patients with new lesions compared to patients without new gadolinium-enhancing lesions at follow-up had a significantly

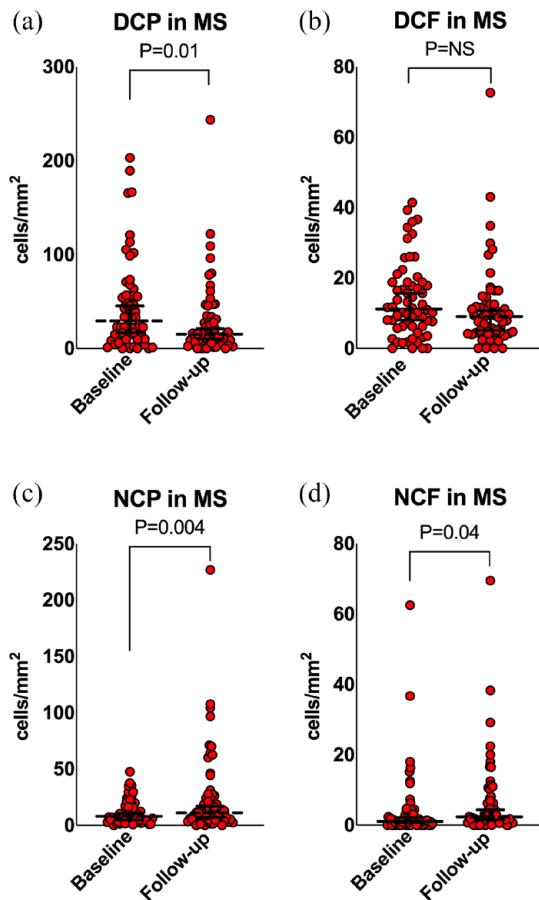


**Figure 5.** Corneal immune cells in patients with MS at baseline compared to follow-up. Graphs represent the median and 95% confidence interval (dashed and continuous black lines respectively) overlaid with the full data range for DCP (a), DCF (b), NCP (c), and NCF (d). Data circles represent data points outside this range for patients with MS (red) at baseline and follow-up. DCF, dendritic cells with fiber contact; DCP, dendritic cells without fiber contact; NCF, non-dendritic cells with fiber contact; NCP, non-dendritic cells without fiber contact; MS, multiple sclerosis.

higher baseline CNBD (37.07, 0.63–73.5,  $p=0.05$ ) with no further differences in clinical, corneal IC parameters, and RNFL at baseline or follow-up.

**Corneal ICs in relation to the history of previous ON.** In patients with MS with previous ON compared to patients who never had ON, baseline EDSS (1.0, 0–1.5,  $p=0.01$ ), baseline and follow-up relapses [(1.0, 0–1.0,  $p=0.007$ ); (1.0, 0–2.0,  $p=0.002$ ) respectively] and baseline and follow-up ARR [(0.94, 0–1.01,  $p=0.01$ ); (0.71, 0.19–1.16,  $p=0.005$ ) respectively] were significantly

higher. There was no significant difference in any of the ophthalmic parameters.

**Corneal IC in relation to disease-modifying treatment status.** At follow-up compared to baseline, 19 (32%) patients with MS switched to a different disease-modifying treatment ( $n=8$ ), restarted ( $n=6$ ), or were off treatment ( $n=5$ ). In patients whose disease-modifying treatment had changed at follow-up compared to patients who were on the same treatment, baseline NCP [1.79, 0.23–10.42,  $p=0.04$ ], and NCF [7.18 (2.56), 2.06–12.29,  $p=0.05$ ] were significantly higher. There were no significant differences in follow-up demographic, clinical, or ophthalmic parameters.

**Corneal IC in relation to baseline interferon.** Patients on interferon at baseline compared to all other patients, excluding patients off treatment, had significantly lower follow-up ARR (0.77, 0–1.32,  $p=0.03$ ) and significantly increased baseline NCP (3.64, –0.21–7.74,  $p=0.05$ ). There was no significant difference in baseline or follow-up relapses, EDSS, MSSS, 25 FWT, CNFD, CNBD, CNFL, RNFL, DCP, DCF, NCF, and follow-up ARR.

**Corneal IC in relation to baseline fingolimod.** Patients on fingolimod at baseline compared to all other patients, excluding patients off treatment, had significantly higher baseline EDSS (3.25, 0–5.5,  $p=0.03$ ) and MSSS (4.54, 0.03–6.09,  $p=0.04$ ) and follow-up EDSS (5.0, 0–6.0,  $p=0.03$ ). There was no significant difference in baseline or follow-up relapses, ARR, 25 FWT, CNFD, CNBD, CNFL, RNFL, DCP, DCF, NCF, and NCP.

**Corneal IC in relation to baseline dimethyl fumarate.** Patients on dimethyl fumarate at baseline compared to all other patients, excluding patients off treatment, had significantly lower follow-up RNFL (–9.71, –18.29 to –1.14,  $p=0.03$ ). There was no significant difference in baseline or follow-up relapses, ARR, 25 FWT, EDSS, MSSS, CNFD, CNBD, CNFL, CNFrD, DCP, DCF, NCF, and NCP.

#### Correlation analysis

Baseline DCP correlated with baseline CNFL ( $r=-0.27$ , –0.50 to –0.01,  $p=0.04$ ), DCF ( $r=0.78$ , 0.66–0.86,  $p<0.0001$ ), NCP ( $r=0.29$ , 0.03–0.51,  $p=0.02$ ); and with follow-up NCF

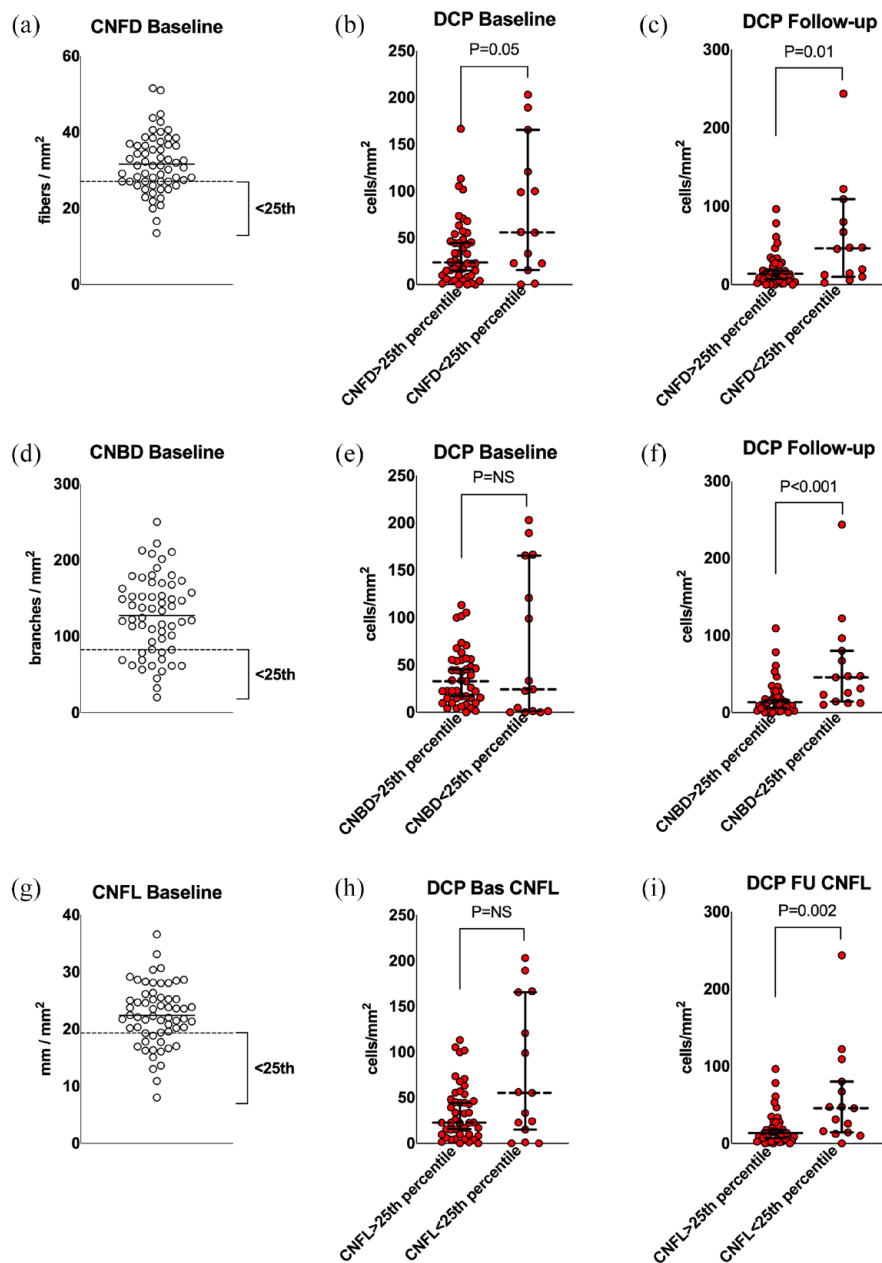


**Figure 6.** DCP at baseline and follow-up for patients with MS with reduced baseline CNFD. Dot plots represent the mean (bold black line) with data points (full range) and 25th percentile (dashed line) for CNFD (a), CNBD (d), and CNFL (g). (b, c, e, f, h, and i) Graphs represent median and 95% confidence interval (dashed and continuous black lines, respectively) overlaid with the full data range for DCP at baseline and follow-up categorized by baseline CNFD, CNBD, and CNFL status, respectively (>25th percentile *versus* <25th percentile).  
CNBD, corneal nerve branch density; CNFD, corneal nerve fiber density; CNFL, corneal nerve fiber length; DCP, dendritic cells without fiber contact; MS, multiple sclerosis.

( $r=0.27$ ,  $0.005-0.49$ ,  $p=0.04$ ) and NCP (both:  $r=-0.27$ ,  $-0.50$  to  $-0.009$ ,  $p=0.04$ ),  
( $r=0.55$ ,  $0.34-0.71$ ,  $p<0.0001$ ). Follow-up CNFL ( $r=-0.29$ ,  $-0.51$  to  $-0.03$ ,  $p=0.02$ ); and  
DCP correlated with baseline CNFD, CNBD with follow-up CNBD ( $r=-0.32$ ,  $-0.53$  to  $-0.06$ ,

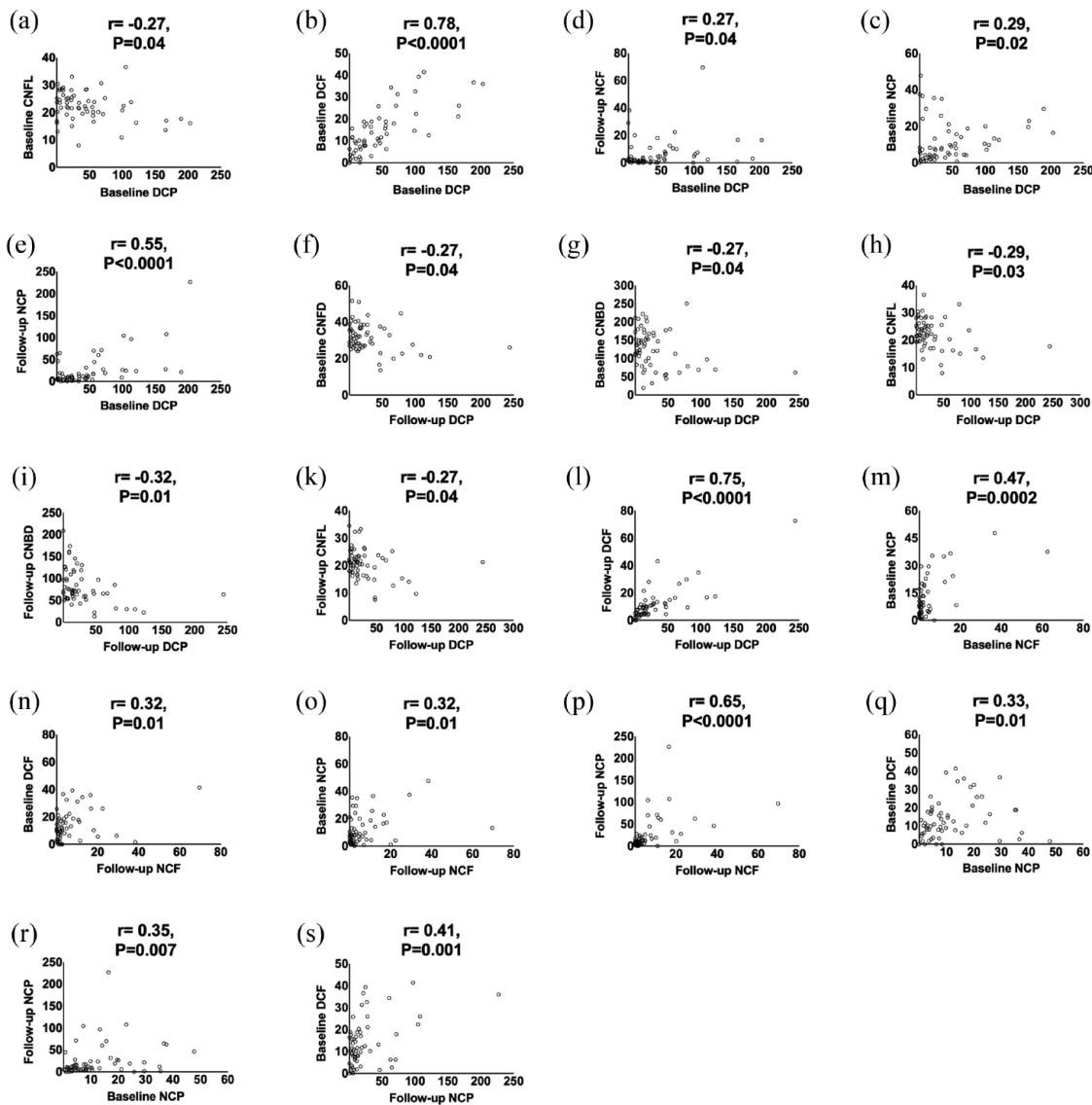


**Figure 7.** Correlation analysis of corneal immune cell parameters (a–s).

$p = 0.01$ ), CNFL ( $r = -0.27$ ,  $-0.50$  to  $-0.01$ ,  $p = 0.04$ ), and DCF ( $r = 0.75$ ,  $0.61$ – $0.85$ ,  $p < 0.0001$ ). Baseline NCF correlated with baseline NCP ( $r = 0.47$ ,  $0.24$ – $0.65$ ,  $p = 0.0002$ ). Follow-up NCF correlated with baseline DCF ( $r = 0.32$ ,  $0.06$ – $0.53$ ,  $p = 0.01$ ) and NCP ( $r = 0.32$ ,  $0.07$ – $0.54$ ,  $p = 0.01$ ); and with follow-up NCP ( $r = 0.65$ ,  $0.47$ – $0.77$ ,  $p < 0.0001$ ). Baseline NCP correlated with baseline DCF ( $r = 0.33$ ,  $0.07$ – $0.54$ ,  $p = 0.01$ ) and follow-up NCP ( $r = 0.35$ ,  $0.09$ – $0.56$ ,  $p = 0.007$ ). Follow-up NCP correlated with baseline DCF ( $r = 0.41$ ,  $0.17$ – $0.61$ ,  $p = 0.001$ ) (Figure 7).

#### Reliability of corneal IC analysis

Intra-rater reliability was excellent for DCF ( $0.96$ ,  $0.89$ – $0.99$ ,  $p < 0.0001$ ), DCP ( $0.98$ ,  $0.95$ – $0.99$ ,  $p < 0.0001$ ), NCF ( $0.99$ ,  $0.98$ – $0.99$ ,  $p < 0.0001$ ), and NCP ( $0.99$ ,  $0.98$ – $0.99$ ,  $p < 0.0001$ ).

#### Discussion

The present study has four main findings. First, DCP and DCF were higher and NCF was lower in patients with RRMS and SPMS compared to healthy controls at baseline and all three parameters showed excellent diagnostic performance to

distinguish between patients with MS and controls. Second, there was a significant decrease in DCP with a significant increase in NCP at follow-up, particularly in RRMS. Third, patients with MS with a lower baseline corneal axonal density had significantly increased DCP at follow-up. Fourth, NCF and NCP were higher and increased during follow-up in patients who switched disease-modifying treatments, and there was a greater increase in NCF at follow-up in patients on interferon treatment.

Inflammation is present during all stages of MS and plays a key role in neurodegeneration<sup>34</sup> as evidenced by axonal loss in both relapsing and progressive MS brain lesions.<sup>35,36</sup> Outside the brain, MS eyes affected by ON exhibit greater retinal axonal loss, compared to the contralateral unaffected eyes, suggesting a similar pathologic pattern.<sup>37</sup> Although current neuroimaging techniques can assess inflammation *in vivo*, methodological issues such as the use of radioligands limits their wider adoption as resourceful endpoints. Corneal axons can be rapidly quantified by CCM and we have previously shown excellent diagnostic performance in diabetic neuropathy and other neurodegenerative disorders.<sup>38</sup> We and others previously demonstrated significant corneal axonal loss in MS,<sup>15-21</sup> which correlated with neurological disability and progressed over time.<sup>16,28</sup> Apart from axons, the cornea also contains corneal ICs, which are immature dendritic cells (MHC-class II, CD80 negative, and/or CD86 negative). These cells act as antigen-presenting cells and form part of the innate immune system. They mediate inflammation by expressing higher levels of MHC-II, and other co-stimulatory molecules such as CD80 and CD86.<sup>39</sup> Apart from molecular alterations, dendritic cells change their volume, sphericity, and motility to elicit adaptive immune responses by priming naive T cells at the draining lymph nodes to effector T cells.<sup>40,41</sup> In a study investigating different models of corneal inflammation, dendritic cell morphology was differentially affected in acute compared to chronic inflammation.<sup>42</sup>

Bitirgen *et al.*<sup>15</sup> first reported increased dendritic cell density in patients with RRMS. Subsequently, we extended these findings to a larger cohort of patients with MS and also demonstrated a correlation with neurological disability and cognitive performance.<sup>29</sup> In the present study, we have used an established protocol<sup>27</sup> from a study in patients

with chronic inflammatory demyelinating polyradiculoneuropathy, whereby cells are categorized into dendritic or non-dendritic types based on size and further subdivided into cells with or without nerve fiber contact. The former measurement allows quantification of cell density while the latter enables quantification of neuroimmune interaction. This is relevant as previous studies have shown that these cells are closely located to nerves during steady state and dissociate during inflammation.<sup>43</sup> Indeed, Stettner *et al.*<sup>27</sup> showed that higher corneal IC density was associated with reduced nerve density in patients with chronic inflammatory demyelinating polyradiculoneuropathy (CIDP) and greater neurological disability and painful symptoms. In a subsequent study, corneal dendritic cell density was higher in patients with CIDP compared to diabetic neuropathy, suggesting that IC assessment could distinguish inflammatory from non-inflammatory neuropathies.<sup>33</sup> Higher dendritic cell density has also been reported in patients with autoimmune dry eye disease compared to non-immune dry eyes, suggesting a relationship with the degree of immune system activation.<sup>44</sup> We report for the first time a significant increase in DCP and DCF in both RRMS and SPMS at baseline, indicating inflammation, that was associated with the severity of corneal nerve loss. Indeed, a DCP > 3.26 cells/mm<sup>2</sup>, a DCF > 4.32 cells/mm<sup>2</sup>, and NCF < 4.58 cells/mm<sup>2</sup> showed excellent diagnostic performance to distinguish controls from patients with MS. Reassuringly, all corneal IC measurements showed excellent intra-rater reliability. A recent study in patients with symptomatic comorbid dry eye disease showed that the presence of more than two dendritic cells was indicative of an underlying autoimmune condition.<sup>45</sup>

There is a lack of natural history data on longitudinal alterations in corneal IC density and morphology. Previously, dendritic cells were shown to decrease following topical<sup>45,46</sup> or systemic<sup>25</sup> anti-inflammatory treatment over 4 weeks to 6 months. In patients with CIDP, a baseline IC count >30 cells/mm<sup>2</sup> had a 100% sensitivity for predicting disease progression over 6 months.<sup>47</sup> In MS, we have previously shown a significant increase in dendritic cells over 2 years in smaller sample of patients with RRMS,<sup>16</sup> while others have recently reported no change in remitting patients over 6 months.<sup>48</sup> In the present study, our results at follow-up suggest that both dendritic and non-dendritic cells undergo dynamic alterations, particularly in RRMS,

independent of newly confirmed relapses. Moreover, these alterations are not related to time while these two morphological subtypes appear to follow opposing trajectories, although they are both associated with a reduction in corneal axonal density at follow-up. Considering that morphological and topographic alterations are hallmarks of corneal IC activity, the present results potentially reflect a pro-inflammatory corneal environment underpinning progressive corneal neurodegeneration.

Increased corneal IC density has been inversely correlated with reduced corneal nerve density<sup>49</sup> in patients with bacterial keratitis and has been related to increased levels of pro-inflammatory cytokines.<sup>50</sup> In systemic disease, the data are currently scarce. A recent study reported a significant increase in dendritic cell density and size in patients with Sjogren's compared to non-Sjogren's dry eye disease, which correlated with disease-specific antibodies.<sup>24</sup> In patients with rheumatoid arthritis, Villani *et al.*<sup>25</sup> reported a marginal increase in dendritic cell density with no difference in corneal nerve morphology. In patients with systemic lupus erythematosus, Bitirgen *et al.*<sup>26</sup> showed a significant reduction in CNBD which correlated inversely with corneal IC density. In our study, patients in the lowest 25th percentile of corneal nerve measures at baseline exhibited a significantly higher DCP density at follow-up, indicating a relationship between corneal axonal loss and immune system activation in patients with MS. Although it is unclear if this effect is systemic or localized, our protocol excluded patients with MS with a history of active ocular disease or prior ocular surgery.

Previous studies have shown that topical or systemic treatment can alter corneal IC density. Topical combination treatment with an immunosuppressant and an anti-inflammatory drug in patients with symptomatic dry eye disease resulted in a significant reduction in dendritic cell density<sup>45</sup> and systemic anti-inflammatory treatment with prednisone in patients with rheumatoid arthritis resulted in a significant reduction in dendritic cell density.<sup>25</sup> Chiang *et al.*<sup>51</sup> reported reduced corneal nerves and a significant increase in immature dendritic cells in patients with cancer treated with oxaliplatin. Corneal dendritic cell density increased dramatically without corneal nerve alterations in a patient with breast cancer

after 11 weeks of treatment with paclitaxel and trastuzumab<sup>52</sup> and then returned to baseline values after cessation of paclitaxel therapy.<sup>53</sup> In the present study, baseline NCF and NCP were higher in patients who switched disease-modifying treatment during follow-up and baseline NCP was higher in patients on interferon. In this context, we hypothesize that higher corneal IC density may reflect reduced treatment effectiveness against underlying inflammation.

We acknowledge certain limitations in our study. First, the relatively short follow-up time does not allow adequate interpretation of our findings in relation to disability worsening. Second, the lack of follow-up in the healthy controls also limits the interpretation of our findings. Third, we did not examine patients immediately after a disease relapse, which would have potentially provided important insights into changes in corneal IC morphology in relation to immune system activation. In summary, we show significant alterations in corneal IC at baseline and follow-up in patients with MS. These alterations are more prominent in patients with lower baseline corneal nerve density, and in those who switch disease-modifying treatments or are on interferon. Future studies need to establish the annualized rate of change in corneal IC morphology and its relationship with markers of systemic inflammation, disease relapses, brain atrophy, and disability worsening.

## Declarations

### *Ethics approval and consent to participate*

This study obtained ethical approvals from the institutional review boards of Weill Cornell Medicine-Qatar (1500064) and Hamad Medical Corporation (15218/15). Participants gave informed written consent to participate in this study.

### *Consent for publication*

Not applicable.

### *Author contributions*

**Ioannis N. Petropoulos:** Data curation; Formal analysis; Funding acquisition; Investigation; Methodology; Project administration; Supervision; Visualization; Writing – original draft.

**Karen John:** Formal analysis; Validation; Writing – review & editing.

**Fatima Al-Shibani:** Formal analysis; Validation; Writing – review & editing.

**Georgios Ponirakis:** Investigation; Writing – review & editing.

**Adnan Khan:** Investigation; Writing – review & editing.

**Hoda Gad:** Investigation; Writing – review & editing.

**Ziyad R. Mahfoud:** Formal analysis; Validation; Writing – review & editing.

**Heba Altarawneh:** Formal analysis; Validation; Writing – review & editing.

**Muhammad Hassan Rehman:** Formal analysis; Validation; Writing – review & editing.

**Dhabia Al-Merekhi:** Formal analysis; Validation; Writing – review & editing.

**Pooja George:** Data curation; Investigation; Project administration; Writing – review & editing.

**Faiza Ibrahim:** Investigation; Project administration; Writing – review & editing.

**Reny Francis:** Investigation; Project administration; Writing – review & editing.

**Beatriz Canibano:** Investigation; Writing – review & editing.

**Dirk Deleu:** Investigation; Writing – review & editing.

**Ahmed El-Sotouhy:** Data curation; Investigation; Writing – review & editing.

**Surjith Vattoth:** Data curation; Investigation; Writing – review & editing.

**Mark Stettner:** Methodology; Writing – review & editing.

**Ahmed Own:** Data curation; Investigation; Resources; Software; Supervision; Writing – review & editing.

**Ashfaq Shuaib:** Investigation; Resources; Supervision; Writing – review & editing.

**Naveed Akhtar:** Investigation; Writing – review & editing.

**Saadat Kamran:** Conceptualization; Funding acquisition; Investigation; Methodology; Resources; Supervision; Writing – review & editing.

**Rayaz A. Malik:** Conceptualization; Funding acquisition; Methodology; Resources; Software; Supervision; Writing – review & editing.

#### *Acknowledgements*

None.

#### *Funding*

The authors disclosed receipt of the following financial support for the research, authorship, and/or publication of this article: This work was supported by the Qatar National Research Fund (grant numbers UREP26-094-3-037, BMRP20038654) and a Merck Grant for Multiple Sclerosis Innovation (grant number 201701.10249.POT). The funders had no role in the study design, data analysis, or manuscript preparation.

#### *Competing interests*

The authors declare that there is no conflict of interest.

#### *Availability of data and materials*

All anonymized, individual-level data used in this manuscript are available to qualified researchers by direct request to the corresponding author. All interested applicants will be asked to sign a data transfer agreement according to institutional regulations prior to receiving any data.

#### **ORCID iDs**

Mark Stettner  <https://orcid.org/0000-0002-8836-0443>

Saadat Kamran  <https://orcid.org/0000-0002-0260-2086>

Rayaz A. Malik  <https://orcid.org/0000-0002-7188-8903>

#### **References**

1. Matthews PM. Chronic inflammation in multiple sclerosis – seeing what was always there. *Nat Rev Neurol* 2019; 15: 582–593.
2. Kutzelnigg A and Lassmann H. Pathology of multiple sclerosis and related inflammatory demyelinating diseases. *Handb Clin Neurol* 2014; 122: 15–58.
3. Alvarez JI, Cayrol R and Prat A. Disruption of central nervous system barriers in multiple sclerosis. *Biochim Biophys Acta Mol Basis Dis* 2011; 1812: 252–264.

4. Wicken C, Nguyen J, Karna R, *et al.* Leptomeningeal inflammation in multiple sclerosis: insights from animal and human studies. *Multiple Scler Relat Disord* 2018; 26: 173–182.
5. Correale J, Gaitán MI, Ysrraelit MC, *et al.* Progressive multiple sclerosis: from pathogenic mechanisms to treatment. *Brain* 2017; 140: 527–546.
6. Tofts PS and Kermode AG. Measurement of the blood-brain barrier permeability and leakage space using dynamic MR imaging. 1. Fundamental concepts. *Magn Reson Med* 1991; 17: 357–367.
7. Absinta M, Vuolo L, Rao A, *et al.* Gadolinium-based MRI characterization of leptomeningeal inflammation in multiple sclerosis. *Neurology* 2015; 85: 18–28.
8. Harrison DM, Li X, Liu H, *et al.* Lesion heterogeneity on high-field susceptibility MRI is associated with multiple sclerosis severity. *Am J Neuroradiol* 2016; 37: 1447–1453.
9. Datta G, Colasanti A, Kalk N, *et al.* 11C-PBR28 and 18F-PBR111 detect white matter inflammatory heterogeneity in multiple sclerosis. *World J Nucl Med* 2017; 58: 1477–1482.
10. Datta G, Violante IR, Scott G, *et al.* Translocator positron-emission tomography and magnetic resonance spectroscopic imaging of brain glial cell activation in multiple sclerosis. *J Mult Scler* 2017; 23: 1469–1478.
11. Pasquini L, Napolitano A, Visconti E, *et al.* Gadolinium-based contrast agent-related toxicities. *CNS Drugs* 2018; 32: 229–240.
12. Betlazar C, Harrison-Brown M, Middleton RJ, *et al.* Cellular sources and regional variations in the expression of the neuroinflammatory marker translocator protein (TSPO) in the normal brain. *Int J Mol Sci* 2018; 19: 2707.
13. Rae CD. A guide to the metabolic pathways and function of metabolites observed in human brain 1H magnetic resonance spectra. *Neurochem Res* 2014; 39: 1–36.
14. Frohman EM, Fujimoto JG, Frohman TC, *et al.* Optical coherence tomography: a window into the mechanisms of multiple sclerosis. *Nat Clin Pract Neurol* 2008; 4: 664–675.
15. Bitirgen G, Akpınar Z, Malik RA, *et al.* Use of corneal confocal microscopy to detect corneal nerve loss and increased dendritic cells in patients with multiple sclerosis. *JAMA Ophthalmol* 2017; 135: 777–782.
16. Bitirgen G, Akpınar Z, Uca AU, *et al.* Progressive loss of corneal and retinal nerve fibers in patients with multiple sclerosis: a 2-year follow-up study. *Transl Vis Sci Technol* 2020; 9: 37.
17. Fernandes D, Luís M, Cardigos J, *et al.* Corneal subbasal nerve plexus evaluation by in vivo confocal microscopy in multiple sclerosis: a potential new biomarker. *Curr Eye Res* 2021; 46: 1452–1459.
18. Mikolajczak J, Zimmermann H, Kheirkhah A, *et al.* Patients with multiple sclerosis demonstrate reduced subbasal corneal nerve fibre density. *J Mult Scler* 2017; 23: 1847–1853.
19. Petropoulos IN, Fitzgerald KC, Oakley J, *et al.* Corneal confocal microscopy demonstrates axonal loss in different courses of multiple sclerosis. *Sci Rep* 2021; 11: 21688.
20. Testa V, De Santis N, Scotto R, *et al.* Neuroaxonal degeneration in patients with multiple sclerosis: an optical coherence tomography and in vivo corneal confocal microscopy study. *Cornea* 2020; 39: 1221–1226.
21. Petropoulos IN, Kamran S, Li Y, *et al.* Corneal confocal microscopy: an imaging endpoint for axonal degeneration in multiple sclerosis. *Investig Ophthalmol Vis Sci* 2017; 58: 3677–3681.
22. Jamali A, Kenyon B, Ortiz G, *et al.* Plasmacytoid dendritic cells in the eye. *Prog Retin Eye Res* 2021; 80: 100877.
23. Jamali A, Lopez MJ, Sendra V, *et al.* Plasmacytoid dendritic cells demonstrate vital neuro-protective properties in the cornea and induce corneal nerve regeneration. *Investig Ophthalmol Vis Sci* 2015; 56: 4355–4355.
24. Hao R, Ding Y and Li X. Alterations in corneal epithelial dendritic cell in Sjogren's syndrome dry eye and clinical correlations. *Sci Rep* 2022; 12: 11167.
25. Villani E, Galimberti D, Del Papa N, *et al.* Inflammation in dry eye associated with rheumatoid arthritis: cytokine and in vivo confocal microscopy study. *Innate Immun* 2013; 19: 420–427.
26. Bitirgen G, Kucuk A, Ergun MC, *et al.* Subclinical corneal nerve fiber damage and immune cell activation in systemic lupus erythematosus: a corneal confocal microscopy study. *Transl Vis Sci Technol* 2021; 10: 10.
27. Stettner M, Hinrichs L, Guthoff R, *et al.* Corneal confocal microscopy in chronic inflammatory demyelinating polyneuropathy. *Ann Clin Transl Neurol* 2016; 3: 88–100.
28. Petropoulos IN, Al-Shibani F, Bitirgen G, *et al.* Corneal axonal loss as an imaging biomarker of neurodegeneration in multiple sclerosis: a longitudinal study. *Ther Adv Neurol Disord* 2023; 16: 17562864221118731.

29. Khan A, Li Y, Ponirakis G, *et al.* Corneal immune cells are increased in patients with multiple sclerosis. *Transl Vis Sci Technol* 2021; 10: 19.
30. Polman CH, Reingold SC, Banwell B, *et al.* Diagnostic criteria for multiple sclerosis: 2010 revisions to the McDonald criteria. *Ann Neurol* 2011; 69: 292–302.
31. Roxburgh RHR, Seaman SR, Masterman T, *et al.* Multiple sclerosis severity score using disability and disease duration to rate disease severity. *Neurology* 2005; 64: 1144–1151.
32. Petropoulos IN, Alam U, Fadavi H, *et al.* Rapid automated diagnosis of diabetic peripheral neuropathy with in vivo corneal confocal microscopy. *Investig Ophthalmol Vis Sci* 2014; 55: 2071–2078.
33. Fleischer M, Lee I, Erdlenbruch F, *et al.* Corneal confocal microscopy differentiates inflammatory from diabetic neuropathy. *J Neuroinflammation* 2021; 18: 89.
34. Campbell GR, Worrall JT and Mahad DJ. The central role of mitochondria in axonal degeneration in multiple sclerosis. *J Mult Scler* 2014; 20: 1806–1813.
35. Frischer JM, Bramow S, Dal-Bianco A, *et al.* The relation between inflammation and neurodegeneration in multiple sclerosis brains. *Brain* 2009; 132: 1175–1189.
36. Ferguson B, Matyszak MK, Esiri MM, *et al.* Axonal damage in acute multiple sclerosis lesions. *Brain* 1997; 120: 393–399.
37. Nolan-Kenney RC, Liu M, Akhand O, *et al.* Optimal intereye difference thresholds by optical coherence tomography in multiple sclerosis: an international study. *Ann Neurol* 2019; 85: 618–629.
38. Petropoulos IN, Bitirgen G, Ferdousi M, *et al.* Corneal confocal microscopy to image small nerve fiber degeneration: ophthalmology meets neurology. *Front Pain Res* 2021; 2: 725363.
39. Hamrah P, Huq SO, Liu Y, *et al.* Corneal immunity is mediated by heterogeneous population of antigen-presenting cells. *J Leukoc Biol* 2003; 74: 172–178.
40. Liu Y, Hamrah P, Zhang Q, *et al.* Draining lymph nodes of corneal transplant hosts exhibit evidence for donor major histocompatibility complex (MHC) class II-positive dendritic cells derived from MHC class II-negative grafts. *J Exp Med* 2002; 195: 259–268.
41. Seyed-Razavi Y, Chinnery HR and McMenamin PG. A novel association between resident tissue macrophages and nerves in the peripheral stroma of the murine cornea. *Investig Ophthalmol Vis Sci* 2014; 55: 1313–1320.
42. Jiao H, Naranjo Golborne C, Dando SJ, *et al.* Topographical and morphological differences of corneal dendritic cells during steady state and inflammation. *Ocul Immunol Inflamm* 2020; 28: 898–907.
43. Jamali A, Seyed-Razavi Y, Chao C, *et al.* Intravital multiphoton microscopy of the ocular surface: alterations in conventional dendritic cell morphology and kinetics in dry eye disease. *Front Immunol* 2020; 11: 742.
44. Kheirkhah A, Dohlman TH, Amparo F, *et al.* Effects of corneal nerve density on the response to treatment in dry eye disease. *Ophthalmology* 2015; 122: 662–668.
45. Levine H, Hwang J, Dermer H, *et al.* Relationships between activated dendritic cells and dry eye symptoms and signs. *Ocul Surf* 2021; 21: 186–192.
46. Villani E, Garoli E, Termine V, *et al.* Corneal confocal microscopy in dry eye treated with corticosteroids. *Optom Vis Sci* 2015; 92: e290–e295.
47. Motte J, Grüter T, Fisse AL, *et al.* Corneal inflammatory cell infiltration predicts disease activity in chronic inflammatory demyelinating polyneuropathy. *Sci Rep* 2021; 11: 15150.
48. Dericioğlu V, Akkaya Turhan S, Erdem HE, *et al.* In vivo corneal confocal microscopy in multiple sclerosis: can it differentiate disease relapse in multiple sclerosis? *Am J Ophthalmol* 2023; 250: 138–148.
49. Cruzat A, Witkin D, Baniyasi N, *et al.* Inflammation and the nervous system: the connection in the cornea in patients with infectious keratitis. *Investig Ophthalmol Vis Sci* 2011; 52: 5136–5143.
50. Yamaguchi T, Calvacanti BM, Cruzat A, *et al.* Correlation between human tear cytokine levels and cellular corneal changes in patients with bacterial keratitis by in vivo confocal microscopy. *Investig Ophthalmol Vis Sci* 2014; 55: 7457–7466.
51. Chiang JCB, Goldstein D, Tavakoli A, *et al.* Corneal dendritic cells and the subbasal nerve plexus following neurotoxic treatment with oxaliplatin or paclitaxel. *Sci Rep* 2021; 11: 22884.
52. Sterenczak KA, Stache N, Bohn S, *et al.* Burst of corneal dendritic cells during trastuzumab and paclitaxel treatment. *Diagnostics* 2021; 11: 838.
53. Bohn S, Stache N, Sperlich K, *et al.* In vivo monitoring of corneal dendritic cells in the subbasal nerve plexus during trastuzumab and paclitaxel breast cancer therapy—a one-year follow-up. *Diagnostics* 2022; 12: 1180.